Large-eddy simulation of flow in a plane, asymmetric diffuser

By Hans-Jakob Kaltenbach

Recent improvements in subgrid-scale modeling as well as increases in computer power make it feasible to investigate flows using large-eddy simulation (LES) which have been traditionally studied with techniques based on Reynolds averaging. However, LES has not yet been applied to many flows of immediate technical interest. This report describes *preliminary* results from LES of a plane diffuser flow. The long term goal of this work is to investigate flow separation as well as separation control in ducts and ramp-like geometries.

1. Motivation and objectives

Flow separation is a fundamental phenomenon which occurs in many engineering flow configurations such as airfoils, diffusers, and cascades. Prevention of separation usually improves the performance of such devices by increasing pressure recovery, enhancing lift, and decreasing total drag. Methods which delay or prevent separation include passive devices like vortex generators and active systems which use auxiliary power to modify the flow. Recent experiments (Katz *et al.* *1989*, Seifert *et al.* 1992, 1993, Obi *et al.* 1993) have shown that flow control strategies which rely on adding small amounts of periodic disturbances (e.g. suction and blowing at specific locations) can delay separation efficiently without consuming large amounts of auxiliary power.

Investigation of unsteady control concepts using numerical simulation requires a method which computes the spatial as well as the temporal evolution of the turbulent fluctuations. Methods based on the Reynolds averaged Navier Stokes equations have difficulty dealing with the unsteadiness which is essential for the control concept. LES seems to be an ideal tool for studying unsteady control because experimental work has shown that the delay of separation is mostly due to the creation of large-scale vortical structures which improve the entrainment of high-speed fluid into separated zones (Katz *et al.* 1989). LES is very likely to adequately describe this physical mechanism at a reasonable cost. Conversely, direct numerical simulation (DNS) would be rather expensive at the Reynolds numbers under consideration.

The use of generalized coordinates largely enhances the range of possible flow configurations accessible for LES. Finite differences are more convenient to use than highly accurate spectral methods for approximation of derivatives. Little is known about the mutual dependency of use of the SGS-model in combination with a numerical scheme with considerable dispersive properties like second order central differences. One way of exploring this dependency consists of studying the sensitivity of the solution with respect to grid resolution.

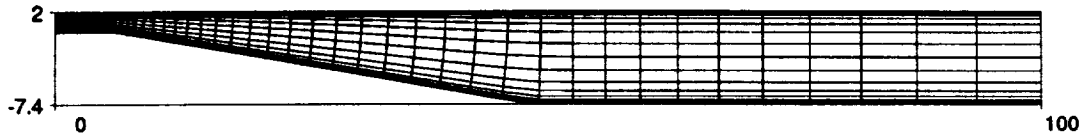

FIGURE 1. Computational domain for the plane diffuser in units of δ. Only each 4th of the wall-normal and each third of the streamwise grid lines are plotted.

The objective of this study is to perform large-eddy simulation of turbulent flow in a one-sided diffuser. The results will be validated by comparison with the experiment of Obi *et al.* (1993). Once the minimum resolution requirements for accurately simulating this flow have been determined, periodic disturbances with various frequencies and amplitudes will be added to the flow as was done in the experiment. The final goal of this study is to understand the physics of flow control through periodic forcing and to determine the parameters (location, frequency, amplitude) that are most efficient in delaying flow separation.

2. Accomplishments

The DNS code of Choi & Moin (1993) has been modified to allow for simulation of inflow/outflow configurations with either no-slip or no-stress conditions at the upper boundary. A detailed description of the coordinate transformation and the numerical scheme is given in Choi *et al.* (1992). The code solves the unsteady, incompressible Navier-Stokes equations in generalized coordinates in two dimensions and a Cartesian equidistant grid in the third (spanwise) direction. The fully-implicit time integration scheme (Crank-Nicholson) uses Newton linearization along with approximate factorization. The time advancement allows rather large time-steps and CFL-numbers. The Poisson solver makes use of the spanwise periodicity of the domain which allows a Fourier transformation in this direction. The remaining 2D problems are solved by using LU decomposition for the first spanwise wavenumber and an iterative solver for higher wavenumbers. The major part of CPU-time needed for advancing the fractional step scheme by one timestep is spent on performing 3-4 Newton iterations per timestep. Depending on the spanwise resolution, the Poisson solver consumes between 10 and 30% of the computational effort.

Unsteady data are specified at the inflow, and a convective boundary condition is applied at the outflow. The upper and lower boundaries are no-slip walls. The data to be specified at the inflow plane of the domain are created in an independent LES of a fully developed channel flow. At each timestep, a cross-section of the velocity field is stored on disk using data reduction to 4 Byte words in order to minimize data storage and input/output time. These channel flow data are subsequently fed into the code which simulates flow through a non-periodic duct configuration.

A simple version of the dynamic SGS model (Germano *et al.* 1991) has been implemented and tested for a periodic channel flow. It makes use of least-square contraction (Lilly 1992) in combination with spanwise averaging. The total viscosity is constrained to be positive through a clipping operation. The test filter is applied

in the spanwise direction and along horizontal lines in the transformed space. No filtering takes place in the wall-normal direction. The SGS-model increases the CPU-time by less than 10% and has no significant effect on memory requirements. A formulation of the SGS-model in generalized coordinates is given in the appendix.

The code has been used for simulation of turbulent flow through a plane, one-sided diffuser. The dimensions of the computational domain are shown in figure 1. The diffuser geometry and the Reynolds number $Re_b = U_b\delta/\nu = 9000$ match the experimental configuration of Obi *et al.* (1993). Here, U_b denotes the bulk velocity of the incoming fully developed turbulent channel flow of height 2δ. The flow from the inlet channel of length 6δ enters an asymmetric diffuser with an expansion ratio of $a = 4.7$. The diffuser and the outlet channel extend over 42δ and 52δ, respectively. The upper wall remains parallel to the inlet channel whereas the lower wall is deflected by approximately 10°. Both corners formed by the inlet and outlet channels with the lower wall are slightly rounded. With a width of 12δ, the aspect ratios of inlet and outlet channel are 1 : 6 and 1 : 1.28, respectively. The experiment had much higher aspect ratios of 1 : 35 and 1 : 7.45 in order to guarantee a two-dimensional core flow free from sidewall effects.

The grid spacing is based on an estimate for the skin friction coefficient as a function of bulk Reynolds number as given by Dean; $c_{f,b} = 0.061 Re_b^{-0.25}$. For $Re_b = 9000$, this relation gives a value $c_{f,b} = 0.0063$, which corresponds to $Re_\tau = u_\tau\delta/\nu = 500$. Therefore, a wall-unit in the inlet section of the diffuser is 0.002δ. Assuming that the flow in the outlet channel will finally evolve into a fully developed channel flow, the wall-unit in the outflow section increases by the expansion ratio, a, to 0.0094δ. Linear stretching of the mesh sizes in the streamwise and wall-normal directions accounts for this increase. The grid with $\Delta x = 0.375\delta$ ($\Delta x^+ = 190$) in the inflow and $\Delta x = 1.25\delta$ ($\Delta x^+ = 133$) in the outflow section has 124 streamwise points. In the wall-normal direction, 64 points are distributed by using hyberbolic tangent stretching. It should be noted, however, that estimates for grid spacing in the outflow section based on wall-units are probably not very relevant because the flow is partially separated. The proper spacing must be verified from sensitivity studies.

For the present flow it would be highly desirable to use "zonal grids" for the spanwise direction. This would allow accurate simulation of the inlet with a fine spanwise grid and with increasingly coarser grids towards the diffuser outlet. However, the spanwise spacing Δz has to remain constant throughout the domain in the present code. The spanwise spacing must be chosen as a compromise between the different requirements in the inflow and the outflow section. Distribution of 64 points over a spanwise extent of 12δ results in $\Delta z^+ = 94$ in the inflow and $\Delta z^+ = 20$ in the outflow section. These estimates are based on $Re_\tau = 500$, which might not be reached everywhere in the actual simulation. The grid is fine enough to resolve near wall streaks with a characteristic spacing of approximately 100 wall-units in the diffuser outlet but certainly too coarse to realistically simulate the flow in the diffuser inlet section. For the purpose of studying the effect of unsteady blowing and suction on the pressure recovery in the rear part of the diffuser, the features

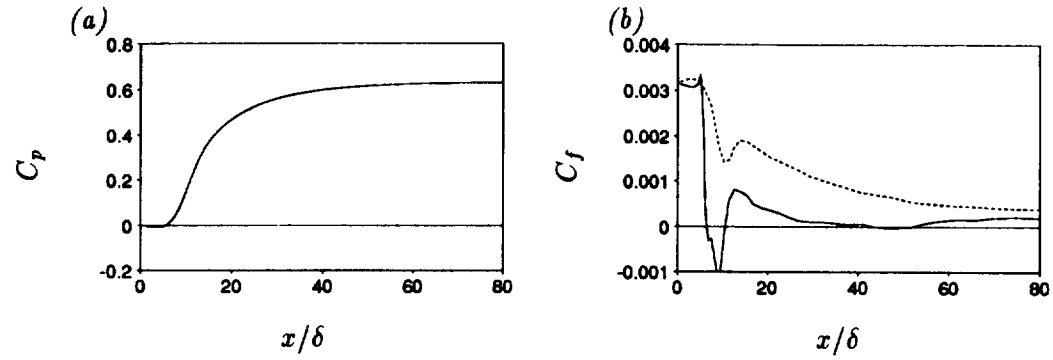

FIGURE 2. (a) Pressure coefficient c_p along the upper wall and (b) skin friction c_f based on centerline velocity at the inflow plane along lower (———) and upper (·····) walls as function of streamwise distance from the inflow plane.

of the flow in the inlet channel might be of minor importance. However, this issue must be tested by means of grid refinement studies.

An estimate of the quality of the simulated inlet flow can be obtained by comparison with Dean's empirical relations for skin friction and ratio of the centerline to the bulk velocity. Dean's correlation $U_c/U_b = 1.27Re_b^{-0.0116}$ gives 1.14 for the Reynolds number considered. Three channel flow LES have been carried out for $Re_b = 9000$ with spanwise spacings $\Delta z^+ = 12, 29$ and 73 based on the *actual* wall shear which changes significantly with the grid resolution. Only the finest case reaches a $c_{f,b} = 0.0064$ ($Re_\tau = 510$), which is close to the value derived from Dean's relation. The other cases reach $c_{f,b} = 0.0054$ ($Re_\tau = 465$) and 0.0038 ($Re_\tau = 393$). This means that the coarsest simulation which is used as database for unsteady inflow underpredicts the skin friction by 40%. However, the values of $U_c/U_b = 1.12, 1.09$ and 1.10 do not differ much between the three cases, indicating that the interior of the flow is well captured by all three simulations. The case with the finest spacing is actually not too far from a DNS because the SGS-eddy viscosity contributes less than 20% to the total viscosity. The plane averaged SGS-eddy viscosity is larger than the molecular viscosity in 60% of the domain in the coarsest case.

The inertial time scale $\tau = 0.5h(x)/U_b(x)$ increases with the square of the expansion ratio from the inlet to the outlet section, i.e. $\tau_{out} = a^2\tau_{in}$. Here, $h(x)$ is the diffuser height at location x. The same holds for the viscous time scale $\tau_{visc} = \nu/u_\tau^2$ which mainly determines the choice of the maximum timestep. Again - as for the spanwise spacing - the choice of the timestep is a compromise between the very different requirements of inlet and outlet section. Running the code with 10 time steps per τ_{in} corresponds to a timestep which is three times bigger than the viscous timescale of the inflow but only one seventh of the viscous timescale of the outflow. In order to obtain converged statistics, data have to be sampled over a period of 100 inertial time scales. Because the inertial timescale of the flow increases by a factor of 22 from inlet to outlet rather long simulation times - of the order of 10000 timesteps - are required.

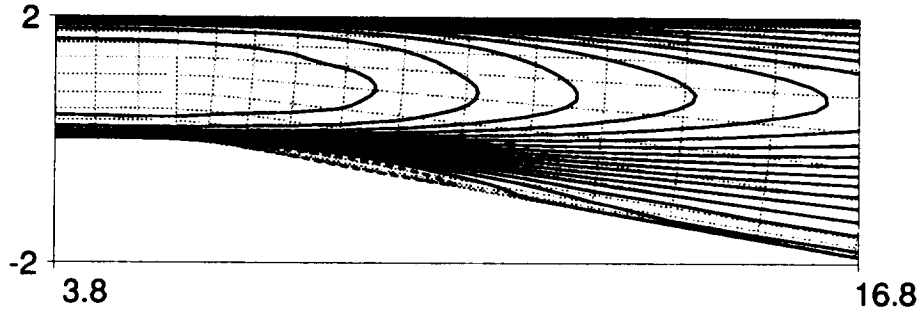

FIGURE 3. Region with reversed flow. Shown are isolines of the contravariant velocity component which is aligned with the horizontal grid lines. The grid lines shown are a subset of the actual grid.

Preliminary results from a coarse grid simulation are shown in figures 2 to 5. Data have been sampled over 300 inlet inertial timescales after running the code for 1000 inlet timescales. Statistics are not fully converged, but the main features of the flow seem to be established.

Figure 2 depicts pressure recovery along the upper wall and skin friction along both walls. Negative values of c_f behind the inlet corner mark the streamwise extent of a first separation bubble. This separated zone, which is shown in more detail in figure 3, was not reported by Obi *et al.* (1993). The flow separation close to the inlet might be an artifact of the coarse spanwise resolution in the diffuser inlet. This can be understood in the following way: the low value of skin friction in the inlet channel indicates that the velocity profile is less full than expected for the given Reynolds number based on centerline velocity. A less full mean velocity profile arises because the turbulent shear stress is underpredicted. Less high speed fluid from the channel core is transported towards the wall which makes separation more likely to occur. Grid refinement studies will be carried out to clarify this point. The skin friction approaches zero in the vicinity of the diffuser outlet. In this region the flow seems to be close to separation. However, we do not find a zone of reversed flow as for the first bubble. In accordance with this finding, mean profiles in the experiment do not show significant backflow at the diffuser outlet.

Profiles of mean velocity and turbulence intensities change drastically inside the diffuser. As described by Simpson (1985), relative high turbulence levels might be found in regions with backflow. Figure 4 shows a strong increase of the streamwise velocity fluctuation in the vicinity of the first separation bubble ($x/\delta \approx 9$). Throughout the rear part of the diffuser, the turbulence intensities remain high compared to the value of the mean velocity (figure 5). The scatter in these profiles is higher than in figure 4 because much longer sampling times are required in the outflow section to obtain converged statistics. There is little evidence from the mean flow profiles that the flow is separated at the diffuser exit.

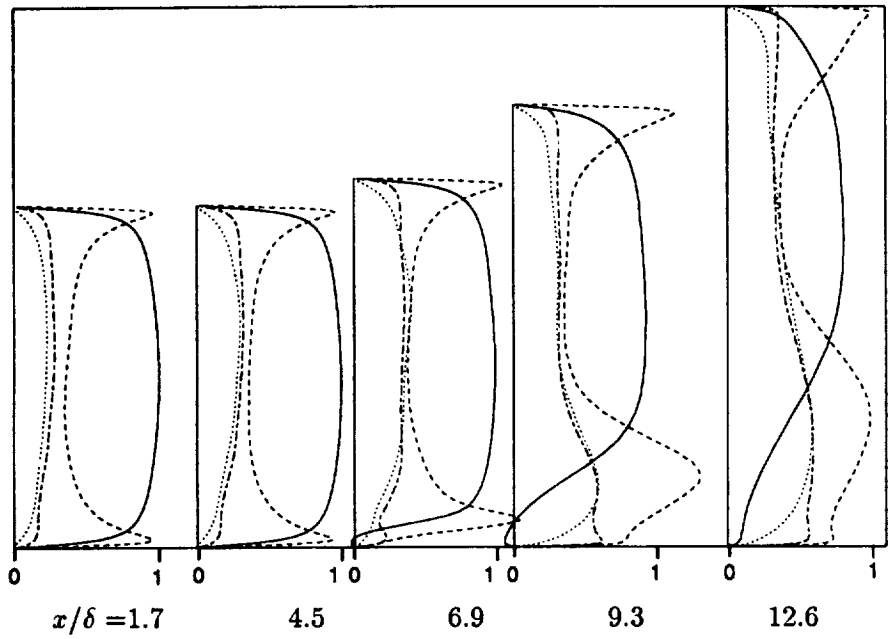

FIGURE 4. Profiles of mean velocity U/U_c (———) and contravariant fluctuations u'/U_c (— — —), v'/U_c (·····) and w'/U_c (— · —) close to the diffuser inlet. Rms-values are enhanced by a factor of five compared to the mean velocity.

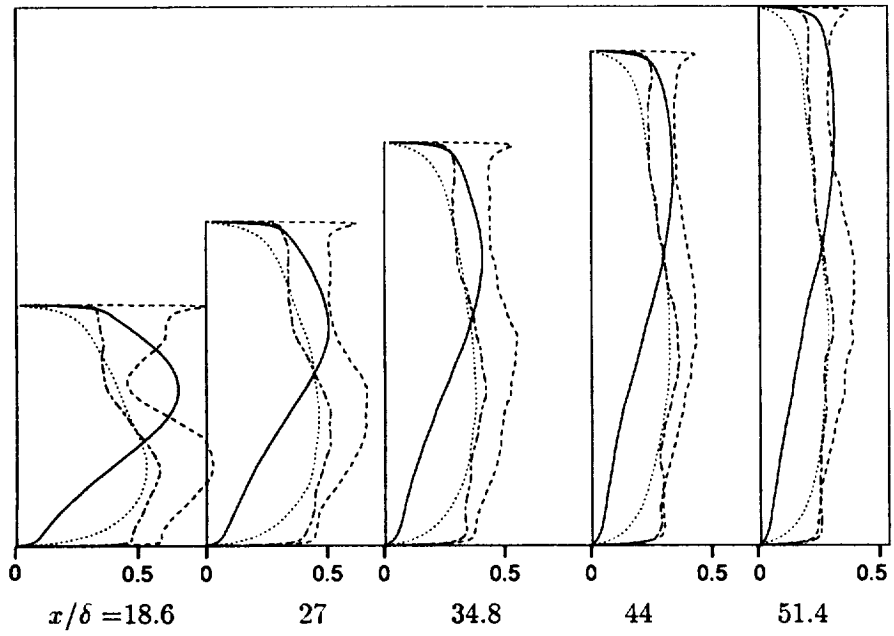

FIGURE 5. Same as figure 4 for the rear part of the diffuser. Note the scale change between this figure and figure 4.

3. Future plans

Grid refinement studies will be carried out in order to see whether underprediction of skin friction in the inlet channel has a significant effect on the flow inside the diffuser. A detailed comparison with available experimental data as well as results from simulations based on statistical turbulence models will be carried out. Once the undisturbed flow is predicted well, oscillatory control of the diffuser will be studied in order to see whether the same gains in pressure recovery are reached in the simulation as in the experiment.

In addition to flow through a diffuser, flow separation at a corner formed by a wall with a hinged rearward facing ramp will be investigated. This configuration resembles the generic flap which is the subject of an ongoing experimental investigation (Seifert *et al.* 1993). The computational domain will be designed such that it matches the experimental configuration of Katz *et al.* (1989). The long term goal of these studies, which are carried out in collaboration with Dr. I. Wygnanski and Dr. A. Seifert, Tel Aviv University, is the improvement of high-lift devices such as highly deflected flaps.

Appendix: The dynamic SGS-model in generalized coordinates

The dynamic model for residual stresses (Germano *et al.*, 1991) requires computation of the Leonard term L^{ij} and the deformation rate tensor S^{ij}. One obtains the scalar model coefficient through contractions of these tensors (and their filtered counterparts). Several possibilities exist to formulate the model in generalized coordinates. If the model formulation is based on a Cartesian system, the Cartesian tensors L^{ij} and S^{ij} have to be computed from the contravariant velocity components. This procedure leads to moderately complex expressions for the components of L^{ij}.

On the other hand, the model can be formulated in generalized coordinates. In this case, contravariant as well as covariant components of strain-rate and Leonard term $\Sigma^{ij}, \Sigma_{ij}, \Lambda^{ij}, \Lambda_{ij}$ have to be evaluated. It turns out that this formulation with certain assumptions leads to rather simple expressions for the Leonard term. This will be shown in the following sections where the definitions

y^i	Cartesian coordinate
x^i	generalized coordinate
v^i	Cartesian velocity component
u^i	contravariant velocity component
$q^i \equiv Ju^i$	velocity component weighted with Jacobian (mesh volume)
$c_i^j \equiv \frac{\partial y^j}{\partial x^i}$	derivative of Cartesian with respect to generalized coordinates
$(c_i^j)^{-1} \equiv \frac{\partial x^i}{\partial y^j}$	derivative of generalized with respect to Cartesian coordinates
$\alpha^{ij} \equiv g^{ij} J$	contravariant metric coefficient weighted with Jacobian

are used.

Starting from the Cartesian formulation for the Leonard term $L^{ij} = \widehat{v^i v^j} - \widehat{v}^i \widehat{v}^j$, where $\widehat{x}$ stands for filtering, the contravariant tensor can be written as

$$\Lambda^{ij} = (c_i^m)^{-1}(c_j^n)^{-1} L^{mn} = (c_i^m)^{-1}(c_j^n)^{-1}(\widehat{v^m v^n} - \widehat{v^m}\,\widehat{v^n})$$

$$= (c_i^m)^{-1}(c_j^n)^{-1}(\widehat{c_p^m u^p c_q^n u^q} - \widehat{c_p^m u^p}\,\widehat{c_q^n u^q})$$

Under the assumption that c_i^j changes only weakly over the distance corresponding to the test filter width, it might be extracted from beneath the filter operator. This leads to

$$\Lambda^{ij} \approx (c_i^m)^{-1}(c_j^n)^{-1} c_p^m c_q^n (\widehat{u^p u^q} - \widehat{u^p}\,\widehat{u^q})$$

$$= \delta_p^i \delta_q^j (\widehat{u^p u^q} - \widehat{u^p}\,\widehat{u^q}) = (\widehat{u^i u^j} - \widehat{u}^i \widehat{u}^j) \quad .$$

Thus, the Leonard term is computed in generalized coordinates from the contravariant velocity components in the same way as L^{ij} from the Cartesian velocity components.

For computation of the strain-rate, the use of non-conservative expressions for derivatives leads to compact expressions. For the purpose of computing the SGS-eddy viscosity, it is probably of little importance whether or not the derivatives are formulated strictly conservative. The code conserves momentum as long as the momentum fluxes over cell surfaces are formulated with a "telescoping" scheme. One obtains the contravariant components Σ^{ij} of the strain rate tensor from

$$\Sigma^{ij} = (c_i^m)^{-1}(c_j^n)^{-1}\frac{1}{2}\left(\frac{\partial v^m}{\partial y^n} + \frac{\partial v^n}{\partial y^m}\right)$$

$$= (c_i^m)^{-1}(c_j^n)^{-1}\frac{1}{2}\left[(c_p^n)^{-1}\frac{\partial v^m}{\partial x^p} + (c_q^m)^{-1}\frac{\partial v^n}{\partial x^q}\right]$$

$$= \frac{1}{2}\left[(c_i^m)^{-1}(c_j^n)^{-1}(c_p^n)^{-1}\frac{\partial v^m}{\partial x^p} + (c_i^m)^{-1}(c_j^n)^{-1}(c_q^m)^{-1}\frac{\partial v^n}{\partial x^q}\right]$$

$$= \frac{1}{2J}\left[(c_i^m)^{-1}\alpha^{pj}\frac{\partial v^m}{\partial x^p} + (c_j^n)^{-1}\alpha^{qi}\frac{\partial v^n}{\partial x^q}\right],$$

where

$$v^m = \frac{1}{J} c_t^m q^t \quad \text{and} \quad v^n = \frac{1}{J} c_s^n q^s$$

has to be inserted because the code is actually formulated in terms of the weighted velocities q^i.

REFERENCES

CHOI, H. & MOIN, P. 1993 The effect of computational timestep on numerical simulation of turbulent flow, to appear in *J. Comp. Phys.*

CHOI, H., MOIN, P. & KIM, J. 1992 Turbulent drag reduction: studies of feedback control and flow over riblets. *Rep. No. TF-55,* Thermosc. Div., Dept. Mech. Engr., Stanford University.

GERMANO, M., PIOMELLI, U., MOIN, P. & CABOT, W. H. 1991 A dynamic subgrid-scale eddy viscosity model. *Phys. Fluids A.* **3,** 1760-1765.

KATZ, Y., NISHRI, B. & WYGNANSKI, I. 1989 The delay of turbulent boundary layer separation by oscillatory active control. *Phys. Fluids A.* **1,** 179-181. Extended version: AIAA paper 89-1027.

LILLY, D. K. 1992 A proposed modification of the Germano subgrid scale closure method. *Phys. Fluids A.* **3,** 2746-2757.

OBI, S., OHIMUZI, H., AOKI, K. & MASUDA, S. 1993 Turbulent separation control in a plane asymmetric diffuser by periodic perturbation; in: *Engineering Turbulence Modelling and Experiments 2*, W. Rodi and F. Martelli (Eds.), Elsevier Science Publ.

SEIFERT, A., BACHAR, T., KOSS, D., SHEPSHELOVICH, M. & WYGNANSKI, I. 1992 Oscillatory blowing, a tool to delay boundary layer separation. *AIAA paper 93-0440*, to be published in AIAA J.

SEIFERT, A., DARABY, A., NISHRI, B. & WYGNANSKI, I. 1993 The effects of forced oscillations on the performance of airfoils. *AIAA paper 93-3264.*

SIMPSON, R.L. 1985 Two-dimensional turbulent separated flow. *AGARDograph 287.*